

Optimal Control of Cellular States

by

Steven Blaber

Dissertation Submitted in Partial Fulfillment of the
Requirements for the Degree of
B.Sc., Simon Fraser University

in the
Department of Physics
Faculty of Science

© Steven Blaber 2017
SIMON FRASER UNIVERSITY
Spring 2017

All rights reserved.

However, in accordance with the *Copyright Act of Canada*, this work may be reproduced without authorization under the conditions for “Fair Dealing.” Therefore, limited reproduction of this work for the purposes of private study, research, education, satire, parody, criticism, review and news reporting is likely to be in accordance with the law, particularly if cited appropriately.

Abstract

Recent experimental advancements have allowed for the precise spatial and temporal control of chemical potentials between proteins in the vicinity of one another through optogenetic techniques [3]. This new technique allows for the investigation of cell signalling. Cells communicate by sending chemical signals to induce changes in chemical potentials which then leads to a change of cellular state. In this thesis we apply non-equilibrium theory [6] to model the response of cells to changes in chemical potential, then, by assuming cells want to minimize wasted energy we derive the optimal protocol for cells to change their cellular state through changes in chemical potential. We provide the theoretical framework to derive this optimal protocol for three separate two state chemical reactions: a discrete open system attached to a bath of proteins, a discrete closed system where the total number of proteins is fixed and a continuous closed system where we consider both the spatial and temporal dependence. Although the theory developed is applicable to these reactions for any transition rates, we assume a specific form which closely resembles cell signalling. The resistance to changes in chemical potential is shown to increase exponentially with chemical potential for an open system, to increase exponentially then decay slowly with chemical potential for a closed system and decreases as $1/r$ where r is the distance from the change. From this we find the optimal protocol and compare the excess work required to change the cellular state using the optimal and naive (constant velocity) protocols. For an open system the optimal protocol is much better than the naive if the chemical potential is varied across a large distance. For a closed system we find similar behaviour for smaller chemical potentials but the improvement then peaks and decreases slowly for very large distances. The spatial dependence of the continuous system has the added effect of decreasing the improvement and smoothing out the peak. We show that our results are consistent with one another in the limiting cases. From this we conclude that cells which require changes in chemical potential within the peak region to change their cellular state will gain the largest benefit from the optimal protocols derived. The optimal protocol has a simple logarithmic form in time $\mu(t) = \ln(ct + b)$, with c and b constants, for the open system, for the closed and continuous systems it has a more complex shape. Proof of concept of directly simulating the system for comparison is shown, and issues with simulation are discussed.

Keywords: Cell Signalling; Optimal Control; Optogenetics; Non-equilibrium Thermodynamics

Acknowledgements

I thank my supervisor, David Sivak (SFU Physics), for the opportunity to work on this project and guidance throughout the process. Also thanks to all the members of the Sivak group at SFU for their insightful comments, and to all the members of the Physics Student Association at SFU for their help and support throughout the entirety of my undergraduate career. This research was enabled in part by support provided by WestGrid (www.westgrid.ca) and Compute Canada Calcul Canada (www.computecanada.ca).

Table of Contents

Abstract	ii
Acknowledgements	iv
Table of Contents	v
List of Figures	vi
1 Introduction	1
2 Theoretical Background	2
2.1 Optimal paths	2
2.2 Poisson representation of chemical reactions and time correlation functions	3
3 Results and Discussion	5
3.1 Discrete model: open system	6
3.2 Discrete model: closed system	10
3.3 Continuous model	13
4 Simulations	17
5 Conclusion	21
Bibliography	23

List of Figures

Figure 3.1	Left: naive excess work (on a semi logarithmic scale) as a function of control parameter distance $\Delta\mu$, for varying unbinding rates k . The naive work increases rapidly, then slows down to an exponential increase in $\Delta\mu$. Right: ratio of naive to optimal works, showing little difference at small distances and increasing with distance.	9
Figure 3.2	A comparison between the friction coefficients for open (black curves) and closed chemical reaction systems (red curves) as a function of chemical potential, at various off rates k . Note that for large k and small μ the two frictions show close agreement.	11
Figure 3.3	Ratio of excess works for both closed (red) and open (black) systems, as a function of control parameter distance, for various unbinding rates k	13
Figure 3.4	Ratio of excess works on a semi-logarithmic scale for closed (red), open (black) and continuous (blue) systems, as a function of control parameter distance, for various unbinding rates k	16
Figure 4.1	Top: simulated fluctuations in particle number for an open chemical reaction system. Bottom: zoomed-in plot of the autocorrelation (normalized by the variance) as a function of lag time.	18
Figure 4.2	Theoretical prediction of the friction coefficient for an open system (red) compared with numerical data (black) demonstrating the noisiness of short-time simulations.	19
Figure 4.3	Top: number fluctuations in an open system, subject to a naive protocol changing chemical potential at a constant rate. Bottom: chemical potential as a function of time.	19
Figure 4.4	Top: number fluctuations in an open system, subject to an optimal protocol changing chemical potential at a rate proportional to $1/t$. Bottom: exponential of chemical potential as a function of time. . .	20

Chapter 1

Introduction

The precise nature of cell signalling is a topic that has long been under investigation. It has been well documented that cells communicate through a language of chemical signals [8]. Our goal is to develop a theory of how a cell can achieve a given signalling outcome at minimal energetic cost. Minimal energetic cost in this case can correspond to a cell using the fewest number of signalling molecules necessary to achieve its goal.

We choose to study the non-equilibrium thermodynamics of cell signalling, and in particular to investigate what optimal signalling looks like. The basic motivation is that life must be out of equilibrium and maintaining these non-equilibrium states has an associated energetic cost. The less energy wasted during operation, the fewer signalling molecules that need to be produced and dynamically secreted at particular times. By modelling biological systems as energetically efficient, we can gain significant insight into the processes by which they may maintain and switch between non-equilibrium steady states and make testable predictions about the behaviour of molecular machines.

Recent experimental advances allow for the precise control of chemical populations in a cell. For example, optogenetic techniques allow for the use of light to adjust, with high spatial accuracy, binding affinity between particular classes of cellular proteins[3]. Since an adjustment of binding affinity changes the chemical potential of one class of proteins in the vicinity of another, it allows for the dynamic implementation of proposed control strategies.

The goal of this project is to characterize the non-equilibrium thermodynamic properties of external changes in chemical potential in simple chemical systems. The framework of optimal control predicts the excess work associated with rapid changes of chemical potential, as a function of system properties such as characteristic length and time scales.

Chapter 2 describes the necessary theoretical background involving optimal control of a system driven out of equilibrium, followed by a description of the stochastic behaviour of both discrete and continuous chemical reactions in the Poisson representation. Later chapters describe the application of this theoretical framework to various simple chemical reaction systems.

Chapter 2

Theoretical Background

We want to predict the work required to rapidly change chemical potential. Toward this goal, we first review a near-equilibrium approximation for this work [6].

2.1 Optimal paths

A physical system at thermal and chemical equilibrium with a reservoir is described by the grand canonical ensemble with free energy

$$\Phi_G \equiv U - TS - \mu N \quad (2.1)$$

for a system with energy U , temperature T , entropy S , chemical potential μ and N particles.

Applying linear response theory [6] gives an expression for the average excess power exerted at a time t' by an external agent, above the average power if the system were equilibrated,

$$P_{ex}(t') = \left[\frac{d\lambda^T}{dt} \right]_{t'} \cdot \zeta[\lambda(t')] \cdot \left[\frac{d\lambda}{dt} \right]_{t'} \quad (2.2)$$

for the generalised friction tensor

$$\zeta_{ij}[\lambda] \equiv \beta \int_0^\infty dt'' \langle \delta f_j(0) \delta f_i(t'') \rangle_\lambda. \quad (2.3)$$

λ is the external control parameter, $f_i \equiv \frac{\partial U}{\partial \lambda}$, and $\langle \delta f_j(0) \delta f_i(t'') \rangle_\lambda$ is the force autocorrelation function defined in terms of equilibrium fluctuations $\delta f_i(t) \equiv f_i(t) - \langle f_i \rangle_\lambda$.

The friction coefficient reflects the increased energy cost as you drive quickly through control parameter space. This leads to an intuitive way of describing the optimal protocol: in areas of high friction you want to drive the system slowly and in areas of low friction quickly.

The integral of the excess power over the control parameter protocol gives the mean excess work

$$W_{\text{ex}} = \int_0^{\Delta t} dt P_{\text{ex}}(t). \quad (2.4)$$

The generalised thermodynamic length,

$$L = \int_0^{\Delta t} dt \sqrt{P_{\text{ex}}(t)}, \quad (2.5)$$

places a lower bound on excess work,

$$W_{\text{ex}} \geq \frac{L^2}{\Delta t}, \quad (2.6)$$

which by the Cauchy-Schwarz inequality is only realized for a protocol with constant excess power. The optimal control parameter protocol between points λ_a and λ_b in fixed time Δt proceeds at a velocity

$$\dot{\lambda}^{\text{opt}} = \frac{(\lambda_b - \lambda_a) \zeta[\lambda(t)]^{-1/2}}{\int_0^{\Delta t} dt' \zeta[\lambda(t')]^{-1/2}}. \quad (2.7)$$

It can be shown that the ratio of the naive (constant velocity) protocol to the optimal protocol can be written in terms of the friction coefficient as [7]

$$\frac{W_{\text{ex}}^{\text{naive}}}{W_{\text{ex}}^{\text{opt}}} = \frac{\bar{\zeta}}{\zeta^{1/2}}. \quad (2.8)$$

The overbar represents the average value over all control parameter points in the protocol.

In this work, the single control parameter is the chemical potential μ . Substituting $\lambda = \mu$ yields $f_i = \frac{\partial U}{\partial \mu} = N$, which implies

$$\langle \delta f_j(0) \delta f_i(t'') \rangle_{\lambda(t'')} = \langle \delta N(0) \delta N(t'') \rangle_{\mu(t'')}. \quad (2.9)$$

Thus from the correlation function of fluctuations in particle number, we can calculate the relevant non-equilibrium thermodynamic quantities for a system of interest.

2.2 Poisson representation of chemical reactions and time correlation functions

The theory described in the previous section says that if we can find the correlations of the fluctuations in the number of particles (or equivalently concentration) we can define all the relevant quantities required for optimal control. Following the derivation for the correlations

between fluctuation in number of particles for a Poissonian or Markovian linearised system in [1] will allow us to express these correlations in a simple form.

A Poisson process gives you the probability of a given number of events occurring in a fixed interval of time and space if these events occur with a known average rate and independently of the time since the last event. A chemical reaction can be treated as one such process.

In the grand canonical ensemble the equilibrium distribution function is

$$P_{\text{eq}}(\mu) = Z^{-1}(\mu) \exp \left[\beta \left(\sum_i \mu_i N_i - E_i \right) \right] \quad (2.10)$$

where $Z(\mu)$ is the grand canonical partition function and N_i is the number of molecules of a certain chemical component i . In an ideal solution the chemical potentials are given by

$$\langle N_i \rangle = C e^{\beta \mu_i} . \quad (2.11)$$

For a linear system (i.e. rates do not depend on square or higher of the concentration) in thermodynamic equilibrium satisfying the above conditions the correlation function has a simple form

$$\langle \delta N_r(t) \delta N_s(t') \rangle_{\text{eq}} = \langle N_r N_s \rangle_{\text{eq}} (\exp[-K_{rs}(t - t')]) , \quad (2.12)$$

with K^{-1} the relaxation time for fluctuations $\langle N(t) \rangle$ and $\langle N_s, N_s \rangle_{\text{eq}}$ the equilibrium covariance. Furthermore, it can be shown that this result is not only limited to Poisson processes but applies to any linear Markov process [4]. A linear Markov process for a chemical reaction is a process whose future outcome depends exclusively on the present state and whose rates do not depend on the square or higher order in concentration.

From this we can now calculate the friction coefficient, excess power, excess work and optimal protocol for a linear Markov or Poisson process.

Chapter 3

Results and Discussion

From Eq. (2.12) and (2.3) we can write the friction coefficient as

$$\zeta_{ij}(\mu) = \beta \int_0^\infty dt'' \langle \delta N_j(0) \delta N_i(t'') \rangle_{\mu(t'')} = \beta \int_0^\infty dt'' \langle N_i N_j \rangle_{eq} (\exp[-K_{ij} t'']) \quad (3.1)$$

assuming K is independent of time and integrating yields

$$\zeta_{ij}(\mu) = \beta \frac{\langle N_i N_j \rangle}{K_{ij}}. \quad (3.2)$$

Now we can write the excess power, work and optimal protocol in terms of the reaction rate K and average number of particles

$$P_{ex}(t) = \left[\frac{d\mu_i^T}{dt} \right]_t \beta \frac{\langle N_i(\mu(t)) N_j(\mu(t)) \rangle}{K_{ij}(\mu(t))} \left[\frac{d\mu_j}{dt} \right]_t. \quad (3.3)$$

This leads to an excess work

$$W_{ex} = \int_0^{\Delta t} dt \left[\frac{d\mu_i^T}{dt} \right]_t \cdot \beta \frac{\langle N_i(\mu(t)) N_j(\mu(t)) \rangle}{K_{ij}(\mu(t))} \cdot \left[\frac{d\mu_j}{dt} \right]_t \quad (3.4)$$

and an optimal protocol which satisfies Eq. (2.7)

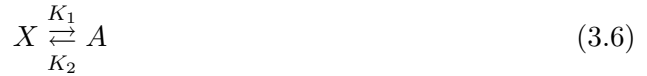
$$\left[\frac{d\mu_i^T}{dt} \right]_t \cdot \beta \frac{\langle N_i(\mu(t)) N_j(\mu(t)) \rangle}{K_{ij}(\mu(t))} \cdot \left[\frac{d\mu_j}{dt} \right]_t = C \quad (3.5)$$

with C an arbitrary constant. Note that in Eq. (3.3)-(3.5) we must include the time dependence of the friction coefficient as the chemical potential is varied meaning the solutions will depend heavily on the choice of system.

3.1 Discrete model: open system

Thus far the discussion has been relatively abstract and general; however, this section will deal with a system specific to cell signalling. Consider a system where a cell signals by sending chemicals which alter the chemical potential between proteins on the cell membrane and freely diffusing proteins in the vicinity of the cell membrane. These proteins will then bind together with a ‘stickiness’ which depends on the chemical potential. This could be through a conformational change, but the details are unimportant for our current analysis. The question we wish to answer is then: how should the signalling cell drive the chemical potential to minimize the excess work (and thus wasted energy)?

To answer this question we first simplify the system to a discrete two-state chemical reaction



where X is the number of proteins bound to the cell membrane and A is the number of freely diffusing proteins. We further simplify the system by assuming the number of freely diffusing proteins is much larger than those attached to the membrane $A \gg N$ and thus $A \approx a = \text{constant}$. This would be true for a large cell and common protein. The rate K_2 of proteins attaching to the membrane will depend primarily on diffusion and not on the strength of the chemical potential. However, we expect the rate K_1 of proteins unbinding the membrane to depend on the chemical potential between the proteins μ as $K_1 = ke^{-\mu}$ since that determines how tightly it is bound.

With these rates the master equation which describes the flow of probability takes the form

$$\partial_t P(x, t) = K_2 a P(x-1, t) + K_1 (x+1) P(x+1, t) - (K_1 x + K_2 a) P(x, t) \quad (3.7)$$

with $P(x, t)$ and abbreviation for $P(x, t|x', t')$ which is the probability of being in state x at time t given that you were in a state x' at time t' . In order to solve this equation we introduce a generating function

$$G(s, t) = \sum_{x=0}^{\infty} s^x P(x, t) . \quad (3.8)$$

Note that by this definition $G(s=1) = \sum_{x=0}^{\infty} P(x, t) = 1$ and the i^{th} factorial moment of x is given by

$$\left\langle \frac{x!}{(x-i)!} \right\rangle = \partial_s^i G(s, t)|_{s=1} . \quad (3.9)$$

Substituting our generating function into the master equation yields

$$\partial_t G(s, t) = K_2 a (s - 1) G(s, t) - K_1 (s - 1) \partial_s G(s, t) . \quad (3.10)$$

Solving this we find that the generating function is [4]

$$G(s, t) = \exp \left[\frac{K_2 a}{K_1} (s - 1) (1 - e^{-K_1 t}) \right] \left[1 + (s - 1) e^{-K_1 t} \right]^N . \quad (3.11)$$

Differentiating with respect to s , then setting $s = 1$ gives us the time dependence of the mean (first factorial moment)

$$\partial_s G(s, t)|_{s=1} = \langle X(t) \rangle = \frac{K_2 a}{K_1} (1 - e^{-K_1 t}) + N e^{-K_1 t} , \quad (3.12)$$

with variance

$$\langle x^2 \rangle - \langle x \rangle^2 = [\partial_s^2 G(s, t) + \partial_s G(s, t) - (\partial_s G(s, t))^2]|_{s=1} = (N e^{-K_1 t} + \frac{K_2 a}{K_1}) (1 - e^{-K_1 t}) . \quad (3.13)$$

Assuming this system is initially at equilibrium, and making use of the fact that it is linear and Markovian we can use Eq. (2.12), with $K = K_1$ and the equilibrium variance corresponding to $t \rightarrow \infty$ in the above equation. Thus

$$\langle \delta X(t) \delta X(0) \rangle_{eq} = \frac{K_2 a}{k e^{-\mu}} (\exp[-k e^{-\mu}(t)]) , \quad (3.14)$$

and by Eq. (3.2)

$$\zeta = \beta \frac{a K_2}{k^2} e^{2\mu} . \quad (3.15)$$

Notice that the friction coefficient depends exponentially on the chemical potential, increases with attachment rate K_2 and decreasing with unbinding rate $K_1 = k e^{-\mu}$. The physical interpretation of this friction as a resistance to motion analogous to viscous drag tells us that in areas of high friction, in order to minimize excess work, we should drive the system slowly. Therefore, as the chemical potential increases you want to decrease the driving velocity. Since the friction depends exponentially on chemical potential, this effect is quite large.

Rearranging Eq. (3.5) allows us to solve for the optimal protocol $\mu^{\text{opt}}(t)$

$$\frac{d\mu^{\text{opt}}}{dt} e^{\mu^{\text{opt}}(t)} = \left[\frac{C k^2}{\beta a k_2} \right]^{1/2} . \quad (3.16)$$

This is a separable equation which can be solved using simple integration to give

$$\mu^{\text{opt}}(t) = \ln \left[t \left(\frac{k^2 C}{\beta a K_2} \right)^{1/2} + C_2 \right] \quad (3.17)$$

$$\dot{\mu}^{\text{opt}}(t) = \left[t \left(\frac{k^2 C}{\beta a K_2} \right)^{1/2} + C_2 \right]^{-1}, \quad (3.18)$$

with C_2 a constant of integration.

In the optimal protocol, as time progresses we drive the system increasingly slow as $1/t$. This is the behaviour we expect based on the friction coefficient derived in Eq. (3.15). As time increases, so does the chemical potential and therefore the friction. The logarithmic form of the optimal chemical potential protocol arises from the exponential dependence of friction on chemical potential, which results in dramatic increases in friction as the system is driven.

Substituting this protocol back into Eq.(3.3) shows that it is indeed constant in time

$$P_{\text{ex}}^{\text{opt}} = \frac{\beta a K_2}{k^2} \quad (3.19)$$

and integrating this gives the excess work

$$W_{\text{ex}}^{\text{opt}} = \Delta t \frac{\beta a K_2}{k^2}. \quad (3.20)$$

To quantify the thermodynamic benefit gained from driving optimally, we compare the work incurred during the optimal protocol, with that during a naive protocol that drives the system at a constant velocity $\dot{\mu}^{\text{naive}} = C_3$. From Eq. (3.4) we find that the naive excess work is

$$W_{\text{ex}}^{\text{naive}} = \frac{C_3 a K_2}{k^2} e^{2C_3 \Delta t}. \quad (3.21)$$

Since we are modelling a biological system which will have a desired initial and final chemical potential, a more useful form of the excess work is as a function of the chemical potential distance $\Delta\mu = \mu_f - \mu_i$ over which the system is driven. By requiring both protocols to drive from an initial to final chemical potential in the same amount of time we can write

$$W_{\text{ex}}^{\text{naive}} = \frac{C_3 \beta a K_2}{2k^2} e^{2\mu_i} (e^{2\Delta\mu} - 1). \quad (3.22)$$

The excess work for the naive protocol depends exponentially on the chemical potential distance the system is driven. This means that changing the chemical potential by large amounts will incur huge energetic costs. Given these huge energetic costs, it seems plausible that living things have devised ways to reduce this cost, as exemplified by driving optimally. The precise amount saved can be most directly quantified by the ratio of the excess works,

given by Eq. (2.8):

$$\frac{W_{\text{ex}}^{\text{naive}}}{W_{\text{ex}}^{\text{opt}}} = \frac{\Delta\mu (e^{2\Delta\mu} - 1)}{2 (e^{\Delta\mu} - 1)^2}. \quad (3.23)$$

A plot of this ratio is shown in Fig. 3.1.

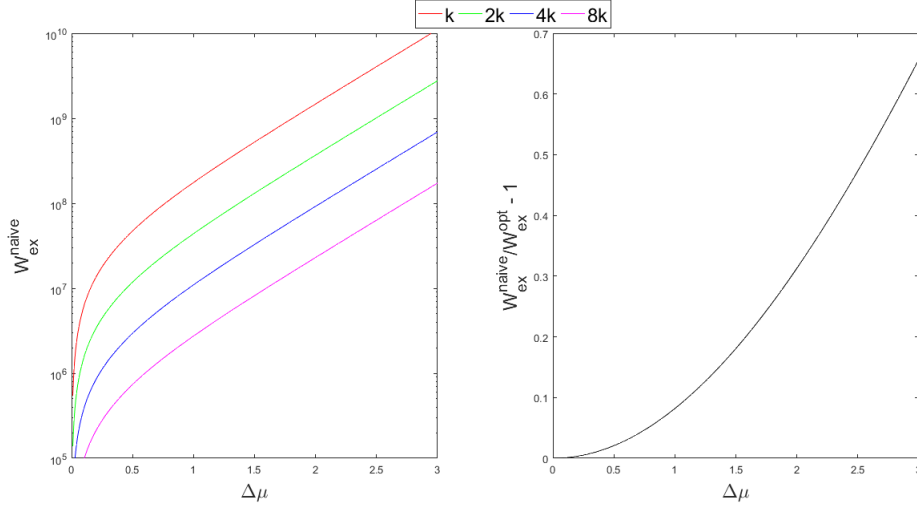


Figure 3.1: Left: naive excess work (on a semi logarithmic scale) as a function of control parameter distance $\Delta\mu$, for varying unbinding rates k . The naive work increases rapidly, then slows down to an exponential increase in $\Delta\mu$. Right: ratio of naive to optimal works, showing little difference at small distances and increasing with distance.

The naive excess work increases very rapidly at small distances due to the $e^{2\Delta\mu} - 1$ term and for large $\Delta\mu$ it increases exponentially. As the chemical potential distance travelled increases, so does the ratio of the excess works. At first this ratio increases rapidly, then settles down to increase linearly with $\Delta\mu$. Since the ratio increases with chemical potential distance, cells that require large changes in chemical potential to achieve their goal will be the ones that benefit the most from using the optimal protocol. Furthermore, since the cost is exponentially increasing in distance, each percentage saved will correspond to a large energy saving, and fewer required signalling molecules.

So far we have assumed that the number of freely diffusing proteins is much greater than the number attached to the cell membrane; however, this will not hold in general. For budding yeast (*Saccharomyces cerevisiae*) the number of copies of proteins per cell can range from as little as 50 to as much as 1300000 [2]. In order to account for this large variability we can expand our analysis to include a system with a fixed total number of proteins in order to cover a wider range of systems.

3.2 Discrete model: closed system

If we assume the total number of proteins is fixed, we can still carry out a similar analysis. The chemical reaction scheme is



Keeping the same rates as before we have $K_1 = ke^{-\mu}$ and K_2 independent of μ . Using the same method as for the open system, we have the master equation

$$\begin{aligned} \partial_t P(x, y, t) = & K_2 y P(x-1, y, t) + K_1 x P(x, y-1, t) + K_1(x+1)P(x+1, y, t) \\ & + K_2(y+1)P(x, y+1, t) - (K_1 x + K_2 y)P(x, y, t) . \end{aligned} \quad (3.25)$$

In order to solve this equation we introduce a two-dimensional generating function

$$G(s, t) = \sum_{x, y=0}^{\infty} (s_1)^x (s_2)^y P(x, y, t) . \quad (3.26)$$

Substituting into our master equation leads to

$$\partial_t G(s_1, s_2, t) = (s_2 - s_1)(K_1 \partial_{s_1} - K_2 \partial_{s_2})G(s_1, s_2, t) . \quad (3.27)$$

Since we expect each of these events (binding, unbinding) to occur independently of the time since the last event we can assume an initially Poissonian distribution. This leads to an initial generating function

$$G(s_1, s_2, 0) = e^{\alpha(s_1-1)+\gamma(s_2-1)} . \quad (3.28)$$

Subject to this initial condition Eq. (3.27) has solutions of the form [4]

$$G(s_1, s_2, t) = \exp \left\{ \frac{K_2 \gamma - K_1 \alpha}{K_1 + K_2} (s_2 - s_1) e^{-(K_1 + K_2)t} + \frac{\alpha + \gamma}{K_1 + K_2} [K_1 (s_2 - 1) + K_2 (s_1 - 1)] \right\} . \quad (3.29)$$

Differentiating with respect to s_1 then setting $s_1 = s_2 = 1$ gives us the time dependence of the mean

$$\langle X(t) \rangle = \partial_{s_1} G(s_1, s_2, t)|_{s_1, s_2=1} \quad (3.30)$$

$$= \frac{k_1 \alpha - K_2 \gamma}{K_1 + K_2} e^{-(K_1 + K_2)t} + \frac{\alpha + \gamma}{K_1 + K_2} K_2 , \quad (3.31)$$

and the variance is

$$\begin{aligned} \langle X^2 \rangle - \langle X \rangle^2 &= [\partial_{s_1}^2 G(s_1, s_2, t) + \partial_{s_1} G(s_1, s_2, t) - (\partial_{s_1} G(s_1, s_2, t))^2] |_{s_1, s_2=1} \\ &= \frac{k_1 \alpha - K_2 \gamma}{K_1 + K_2} e^{-(K_1 + K_2)t} + \frac{\alpha + \gamma}{K_1 + K_2} K_2 . \end{aligned} \quad (3.32)$$

This reaction is linear and Poissonian and thus satisfies all the criteria for Eq. (2.12) with $K = K_1 + K_2$, an equilibrium mean value $\langle X \rangle_{eq} = K_2 N / (K_1 + K_2)$, and variance $\langle x^2 \rangle_{eq} = K_2 N / (K_1 + K_2)$. This leads to a correlation

$$\langle \delta X(t) \delta X(0) \rangle_{eq} = \frac{K_2 N}{K_2 + k e^{-\mu}} \exp[-(k e^{-\mu} + K_2)t] , \quad (3.33)$$

and by Eq.(3.2) a friction coefficient

$$\zeta = \beta \frac{K_2 N}{(K_2 + k e^{-\mu})^2} . \quad (3.34)$$

The friction for a closed system has a similar form to the open system. They both increase exponentially as $e^{2\mu}$ for small values of μ ; however, there is one important distinction. For very large values of chemical potential, the friction for this closed system approaches a constant βN whereas the friction in the open system continues to increase exponentially. A comparison of the two is shown in Fig. 3.2.

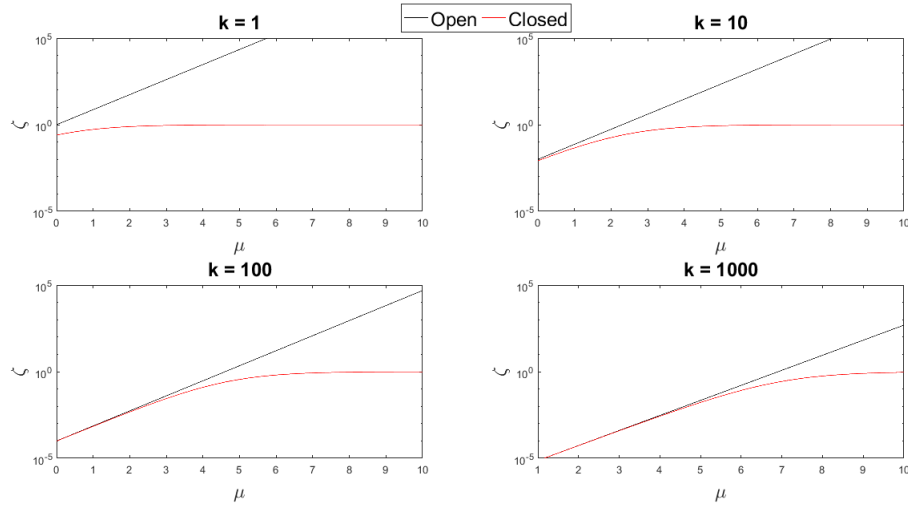


Figure 3.2: A comparison between the friction coefficients for open (black curves) and closed chemical reaction systems (red curves) as a function of chemical potential, at various off rates k . Note that for large k and small μ the two frictions show close agreement.

The friction for the open system is always larger than for the closed system. As k increases the two frictions agree better, because increasing k reduces the time each protein spends attached to the membrane, which if k is very large acts to maintain the number of

freely diffusing proteins constant. This is exactly the assumption made for the open system, so naturally in this limiting case the closed system converges to the open system. However at high chemical potentials, even for large k the unbinding rate is reduced and we no longer see agreement between the two systems.

Rearranging Eq. (3.5) solves for the optimal protocol $\mu(t)$

$$\left[\frac{d\mu(t)}{dt} \right] (K_2 + ke^{-\mu(t)})^{-1} = \sqrt{\frac{C}{\beta K_2 N}}, \quad (3.35)$$

which is a separable equation that can be solved using simple integration to give

$$\mu(t) = \ln \left[\frac{C_3}{K_2} \exp \left[K_2 t \sqrt{\frac{C}{\beta K_2 N}} \right] - \frac{k}{K_2} \right], \quad (3.36)$$

with C_3 a constant of integration. Note that for small times this protocol goes logarithmically in time and is very similar to the optimal protocol for an open system. This is because for small values of μ the friction for the closed and open systems is similar (as time progresses the chemical potential is being increased). For large times this protocol asymptotes to the naive protocol.

From the optimal protocol we can calculate the excess power

$$P_{\text{ex}}^{\text{opt}} = \sqrt{\frac{CN\beta}{K_2}} \quad (3.37)$$

and excess work

$$W_{\text{ex}}^{\text{opt}} = \sqrt{\frac{CN\beta}{K_2}} \Delta t. \quad (3.38)$$

Once again, comparing with the naive protocol gives the ratio of excess works from Eq. (2.8),

$$\frac{W_{\text{ex}}^{\text{naive}}}{W_{\text{ex}}^{\text{opt}}} = \frac{\Delta\mu}{[\ln(K_2 e^{\Delta\mu} + k) - C_2^{\text{int}}]^2} \left[\frac{(K_2 e^{\Delta\mu} + k) \ln(K_2 e^{\Delta\mu} + k) + k}{K_2 e^{\Delta\mu} + k} - C_1^{\text{int}} \right] \quad (3.39)$$

with constants

$$C_1^{\text{int}} = \frac{(K_2 + k) \ln(K_2 + k) + k}{K_2 + k} \quad (3.40)$$

$$C_2^{\text{int}} = \ln(K_2 + k). \quad (3.41)$$

Figure 3.3 shows a plot of this ratio, as well as a comparison with the ratio for an open system.

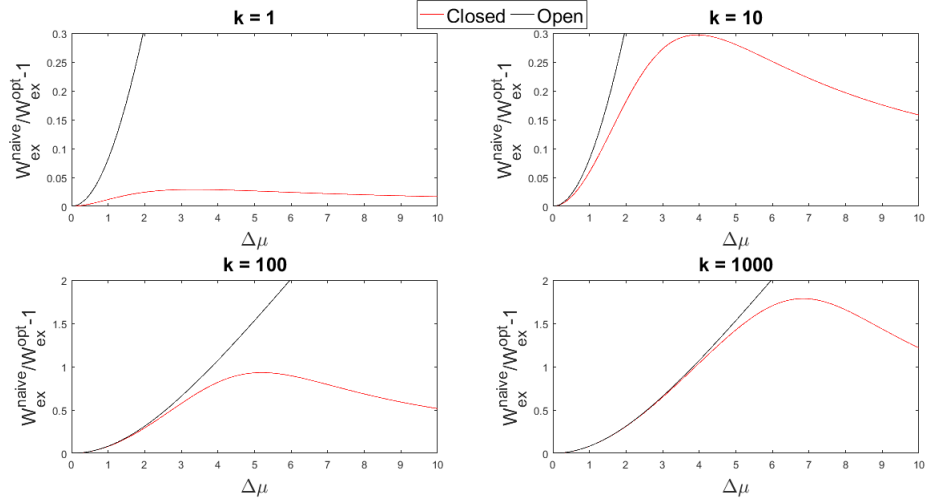


Figure 3.3: Ratio of excess works for both closed (red) and open (black) systems, as a function of control parameter distance, for various unbinding rates k .

In Fig. 3.3 we see the same trend as for the friction, for large values of k and low values of μ . However, as $\Delta\mu$ increases the ratio for the closed system reaches a maximum then slowly falls off to 0 as $\Delta\mu / \ln[e^{\Delta\mu} + k] - 1$. This behaviour is expected: for small times the closed system's optimal protocol is similar to that of the open system, and for large times it asymptotes to the naive protocol. The peak implies that there is a range of distances where the benefit from following the optimal protocol is maximized. The decay of the ratio is slow, so for large chemical potential changes there is still a substantial advantage in using the optimal protocol.

These first two systems have dealt with the case of proteins binding to the cell membrane. This analysis could also apply to two types of freely diffusing proteins in a cell which then bind together. Since before it was assumed that proteins were bound to the cell membrane, we did not consider any information about the spatial distribution of the proteins. In the next section we explicitly account for this spatial dependence.

3.3 Continuous model

If we consider two proteins that can freely diffuse in the cell, and allow for changes in the chemical potential between proteins in the vicinity of one another, we can perform a similar analysis. Since both proteins are free to diffuse we need to consider the spatial distribution of the proteins. This system can be represented by a simple chemical reaction



where X represents the number of proteins bound together, Y the number of unbound proteins and B a constant bath of chemicals to which Y binds to create X such that the only effect of B is to alter the constant rate K_2 . Once again we assume the binding rate K_2 is independent of the chemical potential and the unbinding rate $K_1 = ke^{-\mu}$ depends on the strength of the chemical potential. For this case we must make a further assumption that the proteins are well mixed, allowing us to assume the rates have no spatial dependence.

Let η be the concentration of X and ϵ be the concentration of Y , then our system is governed by the equations

$$\begin{aligned}\partial_t \eta(r, t) &= D\nabla^2 \eta - K_1 \eta + K_2 \epsilon \\ \partial_t \epsilon(r, t) &= D\nabla^2 \epsilon + K_1 \eta - K_2 \epsilon\end{aligned}\tag{3.43}$$

where we have assumed both X and Y have the same diffusion coefficient D . We can further define the stationary two-time correlation matrix $H(r, t)$ as

$$H(r, t) = \begin{bmatrix} \langle \eta(r, t), \eta(0, 0) \rangle & \langle \epsilon(r, t), \eta(0, 0) \rangle \\ \langle \eta(r, t), \epsilon(0, 0) \rangle & \langle \epsilon(r, t), \epsilon(0, 0) \rangle \end{bmatrix}\tag{3.44}$$

and since the system is a linear reaction this leads to

$$\partial_t H(r, t) = \begin{bmatrix} D\nabla^2 - K_1 & K_2 \\ K_1 & D\nabla^2 - K_2 \end{bmatrix} H(r, t).\tag{3.45}$$

The solution can be obtained by Fourier transforming and solving the resultant first-order differential equation matrix. Assuming the system is initially at equilibrium the solution is [4]

$$H(r, t) = \left(\frac{N}{(K_1 + K_2)^2} \right) \frac{e^{-r^2/4Dt}}{(4\pi Dt)^{3/2}} \begin{bmatrix} K_2^2 + K_1 K_2 e^{-(K_1 + K_2)t} & K_1 K_2 (1 - e^{-(K_1 + K_2)t}) \\ K_1 K_2 (1 - e^{-(K_1 + K_2)t}) & K_1^2 + K_1 K_2 e^{-(K_1 + K_2)t} \end{bmatrix},\tag{3.46}$$

with N the total average concentration $\langle \epsilon \rangle + \langle \eta \rangle$. Integrating these correlations gives us the friction tensor at a distance r from the position we perturb the chemical potential

$$\zeta_{ij}(r) = \frac{\beta N}{4\pi D (K_1 + K_2)^2} \begin{bmatrix} \frac{(K_2)^2}{r} + \frac{K_1 K_2}{\sqrt{r^2 + 4D(K_1 + K_2)}} & K_1 K_2 \left(\frac{1}{r} - \frac{1}{\sqrt{r^2 + 4D(K_1 + K_2)}} \right) \\ K_1 K_2 \left(\frac{1}{r} - \frac{1}{\sqrt{r^2 + 4D(K_1 + K_2)}} \right) & \frac{(K_1)^2}{r} + \frac{K_1 K_2}{\sqrt{r^2 + 4D(K_1 + K_2)}} \end{bmatrix}.\tag{3.47}$$

For our analysis we are only considering controlling chemical potential of X , so we are only concerned with correlations in η . Substituting $K_1 = ke^{-\mu}$ yields

$$\zeta_{11}(r) = \frac{\beta N K_2 e^{2\mu}}{(k + K_2 e^\mu)^2} \left[\frac{K_2}{4\pi D r} + \frac{ke^{-\mu}}{4\pi D \sqrt{r^2 + 4D(ke^{-\mu} + K_2)}} \right]. \quad (3.48)$$

The first factor in this friction is identical to the friction we saw for the discrete closed system. The factor in brackets represents the added correction from including the spatial dependence. This friction tells us how much each point a distance r away resists a change in chemical potential at the origin, falling off as $1/r$ with increasing distance from the site of chemical potential change.

By integrating over a sphere of radius R we find the total friction to be

$$\zeta = \frac{\beta N K_2}{(ke^{-\mu} + K_2)^2} \left[\frac{K_2 R^2}{2D} + ke^{-\mu} \left[\frac{R}{2D} \sqrt{4D(ke^{-\mu} + K_2) + R^2} - 2(ke^{-\mu} + K_2) \ln \left[\frac{R + \sqrt{4D(ke^{-\mu} + K_2) + R^2}}{\sqrt{4D(ke^{-\mu} + K_2)}} \right] \right] \right]. \quad (3.49)$$

This result simplifies when R is very large, giving

$$\zeta \approx \frac{\beta N R^2 K_2}{2D(ke^{-\mu} + K_2)} \text{ for } K_2 R^2 \gg D \text{ \& } K_1 R^2 \gg D. \quad (3.50)$$

This approximation assumes that the rate of diffusion is much slower than the total rate of binding/unbinding in the entire cell. This is the assumption we will be using for the remainder of our analysis.

Rearranging Eq. (3.5) gives

$$\frac{d\mu}{dt} (K_2 + ke^{-\mu})^{-1/2} = \sqrt{\frac{2DC}{\beta K_2 N R^2}}, \quad (3.51)$$

which can be solved to give the optimal protocol velocity

$$\mu^{\text{opt}}(t) = \ln \left[\frac{(K_2 k - e^{\tilde{C}t})^2}{4(K_2)^2 e^{\tilde{C}t}} \right] \quad (3.52)$$

$$\tilde{C} = \sqrt{\frac{2DC}{\beta N R^2}}. \quad (3.53)$$

From Eq. (2.8), the ratio of naive to optimal works is

$$\frac{W_{\text{ex}}^{\text{naive}}}{W_{\text{ex}}^{\text{opt}}} = \frac{\Delta\mu(\ln[K_2 e^{\Delta\mu} + k] - C_1^{\text{int}})}{4[\ln[(K_2(K_2 e^{\Delta\mu} + k))^{1/2} + K_2 e^{\Delta\mu/2}] - C_2^{\text{int}}]^2} \quad (3.54)$$

$$C_1^{\text{int}} = \ln[K_2 + k] \quad (3.55)$$

$$C_2^{\text{int}} = \ln[(K_2(K_2 + k))^{1/2} + K_2] . \quad (3.56)$$

Fig. 3.4 shows a plot of this ratio, as well as a comparison with the ratio for open and closed discrete systems.

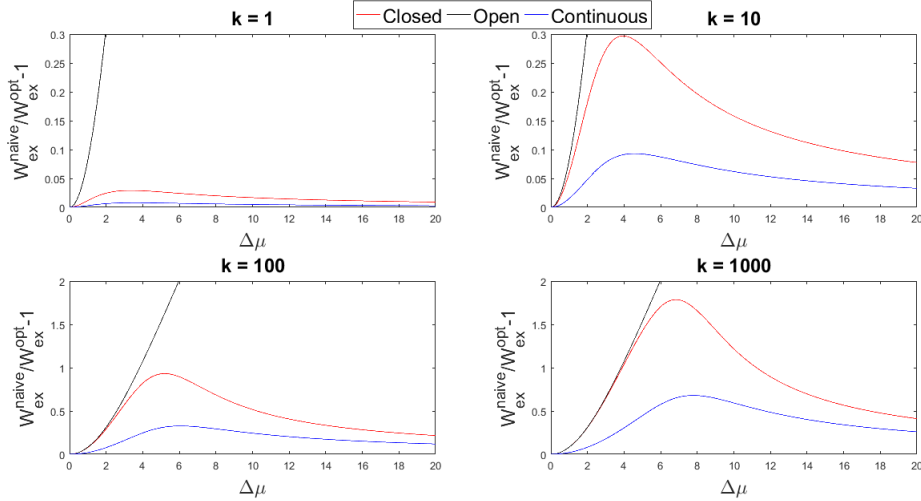


Figure 3.4: Ratio of excess works on a semi-logarithmic scale for closed (red), open (black) and continuous (blue) systems, as a function of control parameter distance, for various unbinding rates k .

Figure 3.4 shows that the continuous system has a similar shape to the closed system but with a smoother peak and decreased amplitude. This effect becomes less pronounced as we increase the unbinding rate k . Like with the closed chemical reaction system, as the unbinding rate increases we return to the approximation of an open system.

We have shown that our results are self consistent: in the limiting cases our more complex models agree with the simpler model. Future work can focus on comparing this theoretical framework with direct simulation and conducting experiments to test the predictions of our theory.

Chapter 4

Simulations

Using the Gillespie algorithm we can simulate the fluctuations in protein number for both the open and closed discrete system in order to determine the validity of the approximations made.

The Gillespie algorithm is a stochastic simulation algorithm used for simulating a multi-state discrete system [5]. With given transition rates between the discrete states, the Gillespie algorithm provides a method of determining the trajectory of the system. For a chemical reaction the process is simple. Start with N particles and a rate k of N increasing, pick a random number r and then after time $\tau = k^{-1} \ln[1/r]$ N increases by 1. This can be done for both rates of N increasing or decreasing, and the choice of which process occurs is selected proportional to their rates. Using a new random number r_2 , a process j which satisfies

$$\sum_{i=1}^{j-1} k_i < r_2 k_{\text{total}} < \sum_{i=1}^j k_i \quad (4.1)$$

is selected. From this we can simulate the fluctuations in the number of particles, as shown in Fig. 4.1.

From the fluctuations in the number of particles we can directly calculate the auto-correlation $\langle \delta N(t), \delta N(0) \rangle$ at a given chemical potential. By numerically integrating this correlation over a sufficiently large time period we can find the friction coefficient as defined in Eq. (2.3). It is at this point we run into numerical issues: in order to get precise results each simulation must be run for millions of time steps, and each simulation gives us the friction at one chemical potential. This type of simulation is very computationally expensive, and the effect is that for limited computation time and memory the data looks noisy, as seen in Fig. 4.2.

We add deterministic driving in order to simulate the naive and optimal protocols, thus simulating fluctuations in particle number while the chemical potential (and therefore the

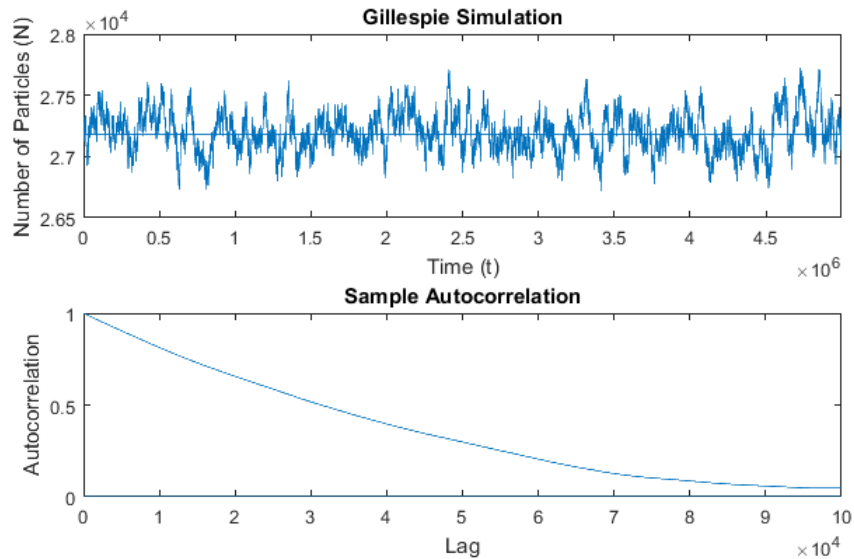


Figure 4.1: Top: simulated fluctuations in particle number for an open chemical reaction system. Bottom: zoomed-in plot of the autocorrelation (normalized by the variance) as a function of lag time.

rate K_1) changes. Figures 4.3 and 4.4 show this driving of the open system for the naive and optimal protocols, respectively.

From these driven simulations we directly calculate the excess work by summing over all the changes in $N\Delta\mu$ to get the total work, then subtracting off the equilibrium work that would have to be done to go from initial to final values of μ .

In order to get precise results from this simulation we would need much longer computation times and memory allocations. This can be done using Compute Canada's Westgrid computer clusters; future work could focus on running these simulations to compare our theoretical work profiles with those directly calculated from simulation for both the open and closed discrete system.

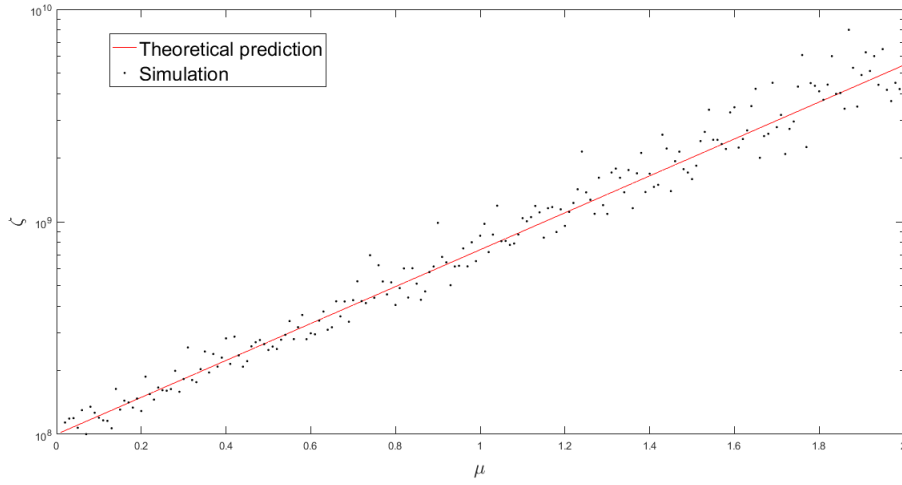


Figure 4.2: Theoretical prediction of the friction coefficient for an open system (red) compared with numerical data (black) demonstrating the noisiness of short-time simulations.

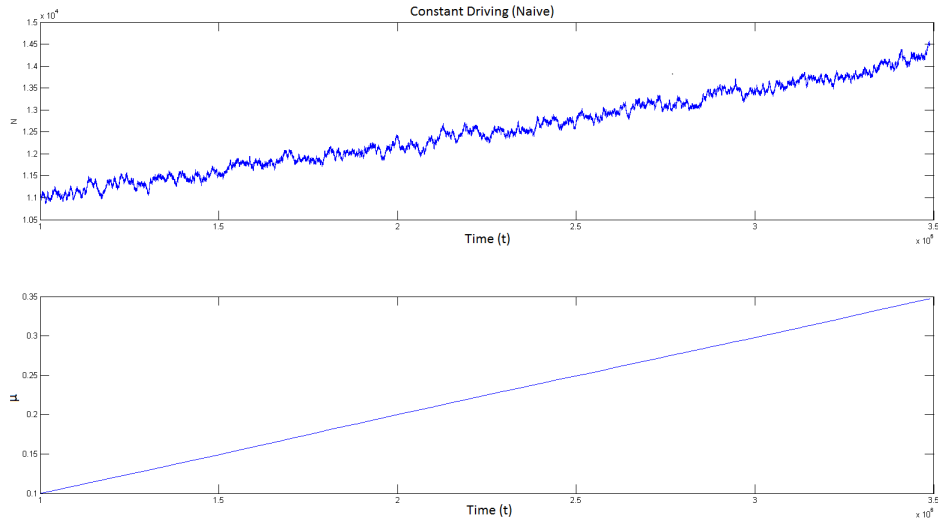


Figure 4.3: Top: number fluctuations in an open system, subject to a naive protocol changing chemical potential at a constant rate. Bottom: chemical potential as a function of time.

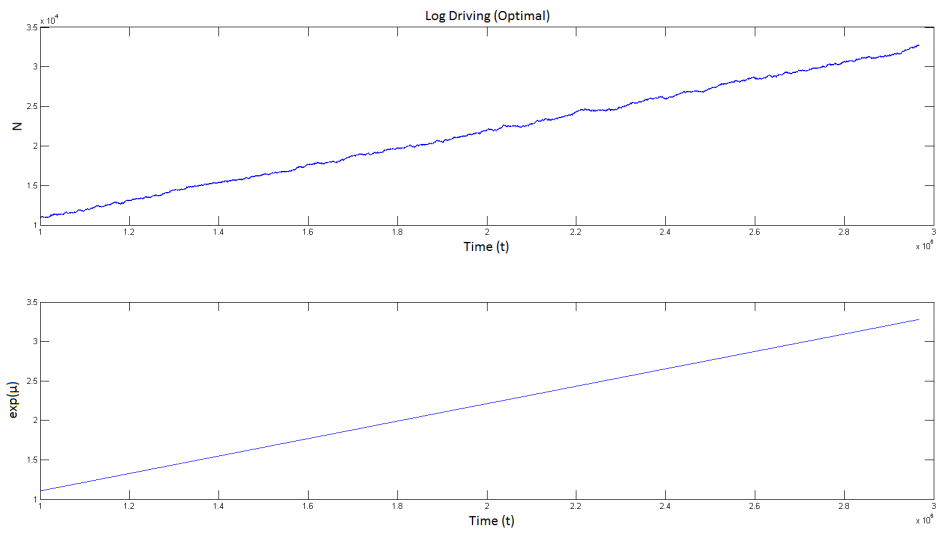


Figure 4.4: Top: number fluctuations in an open system, subject to an optimal protocol changing chemical potential at a rate proportional to $1/t$. Bottom: exponential of chemical potential as a function of time.

Chapter 5

Conclusion

By assuming cells want to minimize the amount of wasted energy when changing between cellular states we were able to model cell signalling using non-equilibrium thermodynamics. Since cell signalling relies on changes in chemical potential we have modelled the cells response to these changes in order to find the optimal signalling protocol. We have developed a theoretical framework for finding the optimal signalling (chemical potential) protocol in three different two state systems: an open system connected to a bath of proteins, a closed system with a fixed total number of proteins and a continuous system where we consider the spatial dependence. These systems correspond to chemical reactions of proteins binding and unbinding at rate which can depend on the chemical potential. We assume that the rate of binding depends primarily on the number of collisions and is independent of the chemical potential, but the rate of unbinding will depend on how strongly they are bound and therefore depends on the chemical potential.

In the open system we have found that the resistance to changes in chemical potential (friction) increases exponentially with chemical potential. As the proteins become more tightly bound any fluctuations in the number of bound proteins will get 'stuck' at that value for longer. This leads to a higher correlation and higher friction. In the closed system we see similar behaviour for low values of chemical potential; however, after a certain point the chemical potential becomes so great that the proteins are unable to unbind and fluctuations decrease, leading to smaller correlation and lower friction. For the continuous case, the resistance to changes in chemical potential decreases as $1/r$ where r is the distance from the point at which you are changing the chemical potential. From this friction we have found the optimal protocols for these three systems: for the open system the optimal protocol goes logarithmically in time $\mu(t) = \ln(ct + b)$, with c and b constants, and for the closed and continuous systems it has a more complex shape. These optimal protocols can give us information about the optimal signalling protocol for cells.

By comparing the excess work from our optimal protocol to the naive (constant velocity) protocol we can determine which biological systems will gain the largest advantage from

the optimal protocol. We find that for an open system, cells that need to drive the chemical potential over a large distance will gain the most benefit from the optimal protocol. For a closed system we find that there is a peak distance where the cell will benefit the most from using the optimal protocol, then this benefit dies off slowly as the distance is increased past this point. Including the spatial dependence smooths out the peak and decreases the benefit gained. From this we conclude that cells that need to drive their chemical potential a distance within the peak region will gain the largest advantage from obeying the optimal protocols derived in this thesis.

We have shown that the Gillespie algorithm can be used to simulate fluctuations in the number of bound particles. This was used numerically calculate the correlation and friction directly from simulation to be compared with theoretical predictions. This system was then driven deterministically to simulate the naive and optimal protocols. With the use of Compute Canada's Westgrid computer cluster we can in principle increase our computation time to acquire accurate simulation data to be compared with the theoretical predictions for excess work.

Optogenetic techniques can be used to control the chemical potentials between light gated proteins which could be used to experimentally test our predictions. This acts as an experimental simulation of cell signalling, and will allow us to see whether or not cells obey the optimal protocols.

Bibliography

- [1] S. Chatuvedi and C.W. Gardiner. The poisson representation. ii. two-time correlation functions. *Journal of Statistical Physics*, 18(5), 1978.
- [2] Huh W.K. et. al. Global analysis of protein expression in yeast. *Nature*, October 2003.
- [3] Zhiping Feng et. al. Optical control and study of biological processes at the single-cell level in a live organism. *Reports on Progress in Physics*, June 2013.
- [4] C.W. Gardiner. *Handbook of Stochastic Methods for Physics, Chemistry and the Natural Sciences*. Springer, 2nd edition, 1985.
- [5] Daniel T. Gillespie. Stochastic simulation of chemical kinetics. *The Annual Review of Physical Chemistry*, October 2006.
- [6] David A. Sivak and Gavin E. Crooks. Thermodynamics metrics and optimal paths. *Physical Review Letters*, May 2012.
- [7] David A. Sivak and Gavin E. Crooks. Thermodynamic geometry of minimum-dissipation driven barrier crossing. *Physical Review E*, November 2016.
- [8] Bruce Mayer Wendell Lim and T. Pawson. *Cell signaling: principles and mechanisms*. Garland Science, Taylor and Francis Group, 1st edition, 2015.